Journal of Rock Mechanics and Geotechnical Engineering 9 (2017) 981–988

Contents lists available at ScienceDirect

Journal of Rock Mechanics and Geotechnical Engineering

journal homepage: www.rockgeotech.org

Full Length Article

Microstructure characteristics of cement-stabilized sandy soil using nanosilica

Asskar Janalizadeh Choobbasti*, Saman Soleimani Kutanaei

Department of Civil Engineering, Babol University of Technology, Babol, Iran

ARTICLE INFO

Article history:
Received 13 November 2016
Received in revised form
6 March 2017
Accepted 8 March 2017
Available online 14 August 2017

Keywords:
Scanning electron microscopy (SEM)
Atomic force microscopy (AFM)
X-ray diffraction (XRD)
Cement
Nanosilica

ABSTRACT

An experimental program was conducted to explore the impact of nanosilica on the microstructure and mechanical characteristics of cemented sandy soil. Cement agent included Portland cement type II. Cement content was 6% by weight of the sandy soil. Nanosilica was added in percentages of 0%, 4%, 8% and 12% by weight of cement. Cylindrical samples were prepared with relative density of 80% and optimum water content and cured for 7 d, 28 d and 90 d. Microstructure characteristics of cement-nanosilica-sand mixtures after 90 d of curing have been explored using atomic force microscopy (AFM), scanning electron microscopy (SEM) and X-ray diffraction (XRD) tests. Effects of curing time on microstructure properties of cemented sandy soil samples with 0% and 8% nanosilica have been investigated using SEM test. Unconfined compression test (for all curing times) and compaction test were also performed. The SEM and AFM tests results showed that nanosilica contributes to enhancement of cemented sandy soil through yielding denser, more uniform structure. The XRD test demonstrated that the inclusion of nanosilica in the cemented soil increases the intensity of the calcium silicate hydrate (CSH) peak and decreases the intensity of the calcium hydroxide (CH) peak. The results showed that adding optimum percentages of nanosilica to cement-stabilized sandy soil enhances its mechanical and microstructure properties.

1. Introduction

Soil treatment with cement agents (e.g. lime, gypsum, Portland cement, and fly ash) has been a ground improvement technique in foundation engineering, road construction, and geotechnical engineering for many years (Choobbasti et al., 2014; Kutanaei and Choobbasti, 2015a,b; Sarokolayi et al., 2015a,b; Tavakoli and Kutanaei, 2015; Mashhadban et al., 2016a). Cementation of sandy soil can result in increasing stiffness, shear strength, compressive strength, and brittle behavior and decreasing compressibility and permeability of the material (Kutanaei and Choobbasti, 2016a; Mashhadban et al., 2016b). The mechanical behavior of cement-treated soil has been explored in the past by several researchers. A number of researches have been performed to investigate the mechanical properties of cement-treated sandy soil using added zeolite, glass, fiber, fly ash, and silica fume in the same manner.

Mola-Abasi and Shooshpasha (2016) investigated the effect of zeolite content on mechanical properties of cemented sandy soil. They found an improvement of compressive strength of cement-treated sandy soil when the cement is replaced by zeolite at an optimum proportion of 30% after 28 d. Al-Swaidani et al. (2016) explored the influence of adding natural pozzolana on geotechnical characteristics of lime-treated clay. The results showed that the geotechnical properties of lime-treated clay are significantly improved when the lime is replaced by natural pozzolana at proportion of 20%. Changizi and Haddad (2015) conducted a series of unconfined compression tests and direct shear tests to explore the effects of nanosilica and fiber on the strength properties of soft clay. They found that the unconfined compressive strength (UCS) and cohesion of clay increase with the increasing nanosilica content.

Limited studies have reported the use of pozzolana such as nanoparticles. The use of nanosilica as cement-based material modifier becomes more popular due to a more satisfactory performance compared with conventional modifiers (e.g. microsilica). Ghazi et al. (2011) performed the unconfined compression tests to study the strength improvement of clay stabilized with 6% cement due to the inclusion of nanosilica. They found that by adding 2%

* Corresponding author.
E-mail address: asskar@nit.ac.ir (A.J. Choobbasti).

Peer review under responsibility of Institute of Rock and Soil Mechanics, Chinese Academy of Sciences.

http://dx.doi.org/10.1016/j.jrmge.2017.03.015

nanosilica, strength is increased from 1.7 MPa to 2.1 MPa. Bahmani et al. (2014) explored the influence of nanosilica particles on the UCS, hydraulic conductivity, and Atterberg limits of cemented clay. They reported that inclusion of nanosilica particles leads to a reduction in plasticity index and an improvement in soil strength. Ghasabkolaei et al. (2016) performed unconfined compression tests and California bearing ratio (CBR) tests to explore the effect of nanoparticles on geotechnical properties of cement-stabilized clayey soil. They found that adding 1.5% nanosilica improves the UCS of the cemented clay. Choobbasti et al. (2015) conducted a series of unconfined compression tests to investigate the mechanical properties of sandy soils stabilized with Portland cement and nanoparticles. They found that the UCS increases with increase in nanosilica content. Kutanaei and Choobbasti (2016a) explored combined impacts of randomly distributed fibers and nanosilica on durability and mechanical characteristics of cement-treated sandy soils. They reported an optimum percentage for the nanoparticles in which the behavior of cement-treated sandy soils reinforced by randomly distributed fiber is improved significantly. Papatzani et al. (2014) investigated the impact of the inclusion of nanosilica on the microstructure characteristics and strength of blended Portland cement pastes. They reported that the microstructure properties of cement paste are improved with adding nanosilica. Papatzani (2016) investigated the impact of nanoparticles on cement hydration. The results showed that the chemical reactivity and durability of the nano-modified cement product are remarkably altered compared to cement pastes. Therefore, nanoparticles can improve the properties of cement.

Review of the literature relating to the mixture of nanosilica and cemented sandy soil shows that no attention has been paid to the use of nanosilica on microstructure of sandy soil. Hence, this research aims to quantify the impacts of the percentage of nanosilica and curing period on the microstructure and UCS of the cement-treated sandy soil. Unconfined compression tests and compaction tests are conducted and the impacts of these variables on the results are investigated. Microstructure characteristics of cement-treated sandy soil with nanoparticles are explored using atomic force microscopy (AFM), scanning electron microscopy (SEM) and X-ray diffraction (XRD) tests.

2. Experimental program

Twelve unconfined compression tests, 4 compaction tests, 8 SEM tests, 4 AFM tests and 4 XRD tests were performed to investigate the effects of nanosilica on the performance of cement-treated sandy soil.

2.1. Materials

Babolsar sand was used in this study. The particle size distribution curve for Babolsar sand is shown in Fig. 1. The ordinary Portland cement of type II was used as cement agent. Its chemical and physico-mechanical characteristics are presented in Tables 1 and 2, respectively. Nanosilica with a solid content of more than 99% was used. Physical characteristics of nanosilica particles are presented in Table 3. Distilled water was used for sample preparation.

2.2. Sample preparation

The undercompaction technique was used for sample (52 mm in diameter and 104 mm in height) preparation in this study based on the method described by Ladd (1978). The requisite amount of oven-dried sand was mixed with the desired amount of Portland cement and nanosilica until uniform color of mixture was achieved (about 30 min), and then the water equal to the optimum water content was added continuously to the mixture and mixed for about 20 min. After mixing process, the mixture was then divided into five portions and stored in a covered container to avoid moisture losses before compaction. Each portion was transferred into a 52 mm in diameter by 104 mm in height split mold and compacted using a metal hammer until the desired height was reached. The top of each layer was scratched before adding the next layer to promote suitable bonding. To control the homogeneity of sample density along height, one sample (for each mixture) was cut by a narrow saw wire at four positions, and the density of each piece has been determined and then the standard division was calculated. The standard division was 0.06 which showed good homogeneity of density. The tests were conducted on the samples with relative density of 80%. Each sample was cured in a humid room at a constant temperature of (25 ± 2) °C and relative humidity of >90% for 7 d, 28 d and 90 d. Before tests, the samples were submerged in distilled water for 1 d for saturation to minimize matric suction. Immediately before the unconfined compression test and microstructure imaging, the samples were removed from the water container and dried with an absorbent cloth.

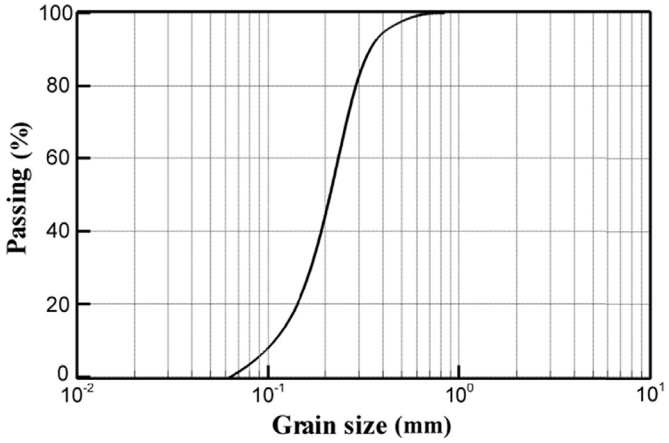

Fig. 1. Particle size distribution curve for Babolsar sand.

Table 1
Chemical compositions of ordinary Portland cement (percentage by weight of cement, wt%).

SiO_2	Al_2O_3	Fe_2O_3	CaO	MgO	SO_3	$CaCO_3$	Loss on ignition
21.9	4.86	3.3	63.33	1.15	2.1	–	2.4

Table 2
Physico-mechanical properties of cement.

Blaine fineness (cm^2/g)	Expansion (autoclave) (%)	Specific gravity	UCS (MPa)		
			3 d	7 d	28 d
3050	0.05	3.1	18.1	28.9	38.9

Table 3
Physical properties of nanosilica particles.

Diameter (nm)	Specific surface area (m^2/g)	Density (g/cm^3)	Purity (%)	Shape
20–40	193	1.7	>99	White powder

2.3. Testing procedures

The unconfined compression tests were performed in accordance with ASTM D2166/D2166M-16 (2016) test method on cemented samples with different curing times (7 d, 28 d and 90 d) and nanosilica contents (0%, 4%, 8% and 12%). The samples were loaded at a displacement rate of 1 mm/min. To assess the validity of the obtained results, three samples were prepared from each mixing design. After each test, the average error was calculated. The test results were considered suitable for presenting if their average error was less than 5%.

To investigate the influences of nanosilica and cement contents on the optimum water content and maximum dry density of treated and untreated sands, standard Proctor compaction tests were done immediately after mixing process in accordance with ASTM D698 (2010). The standard Proctor compaction tests were repeated on three identical mixtures. The average value of obtained results was then used.

XRD analyses of nanosilica-cement-sand and cement-sand mixtures after 90 d of curing were carried out using a Philips PW 3710 diffractometer. XRD curves were obtained using a Cu Kα radiation (l.5148 Å) with a voltage of 30 kV and a current setting of 30 mA. Air-dried powdered samples of nanosilica-cement-sand and cement-sand mixtures were analyzed. The scan step size 2θ ranges from 10° to 60°. The XRD measurements were conducted with a step of 0.02°.

To explore the microstructure of the nanosilica-cement-sand and cement-sand mixtures, some of the samples were obtained from the central part of the unconfined compression test samples. The Hitachi S-4160 was used for morphological investigations of the nanosilica-treated and untreated cemented sand matrix. Before imaging, the SEM samples mounted on aluminum stubs were coated with gold for better conductivity. The magnification of the SEM photos is about 30,000 times. The SEM instrument was operated at 10 kV.

The surface topography of the cemented sand sample after 90 d of curing with different nanosilica contents was explored by using AFM (model: easyscan2 flex AFM, Swiss) imaging. The AFM samples were obtained from the central part of the unconfined compression test samples. Surface topography of prepared samples was imaged in a scanning size of 5 μm × 5 μm.

3. Results and discussion

3.1. Compaction

The impacts of nanosilica and cement contents on the optimum water content and maximum dry density of sandy soil are presented in Fig. 2. It can be seen that the addition of Portland cement to the sandy soil increases its maximum dry density. This behavior may be attributed to the presence of large, high-density (high specific gravity) aggregate particles. Moreover, Portland cement has finer particles rather than sandy soil; hence, the pore within the coarse aggregate becomes occupied by Portland cement grains and makes a denser structure with higher maximum dry density. Fig. 2 also shows that there is a low decreasing rate in the maximum dry density with increasing percentage of nanoparticles for low nanosilica content (up to 4%). The increase in maximum dry density of cemented sand mixed with nanosilica can be explained by the fact that the void within the aggregate becomes occupied by nanoparticles. In the case of high nanosilica content (4%–8%), since nanoparticles have a lower specific gravity (1.7) compared to sand grains (2.78), the maximum dry density decreases after certain nanosilica content. As presented in Fig. 2, the optimum water content of cemented sandy soil sample increases with the increase

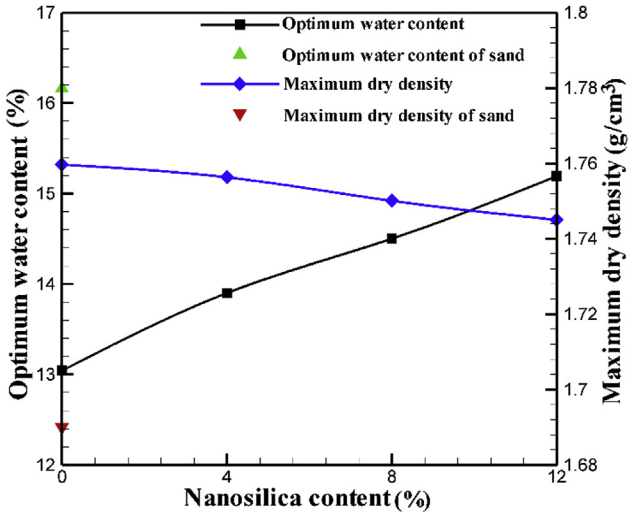

Fig. 2. Effects of nanosilica and cement contents on the optimum water content and maximum dry density.

in nanosilica content. This behavior can be explained by the fact that the nanoparticles provide more susceptible area and require more water to hydrate.

3.2. Unconfined compression test and microstructure imaging

3.2.1. Effect of nanosilica content

The impact of nanosilica content on the UCS and UCS ratio (the UCS of sample was normalized to the UCS at 7 d of curing) of samples is shown in Fig. 3. The obtained results show that for cemented sand, when the nanosilica content is increased to an optimum amount of 8%, the UCS of samples is significantly improved and then decreases with increase in nanosilica content from 8% to 12%. The improvement of UCS of the cemented sand sample containing nanosilica is due to the rapid consumption of calcium hydroxide (CH) formed during hydration process of cement agent, which is related to the high reactivity of nanosilica particles. Comparison of the present results with published results reveals that the high nanosilica content is obtained as the optimum

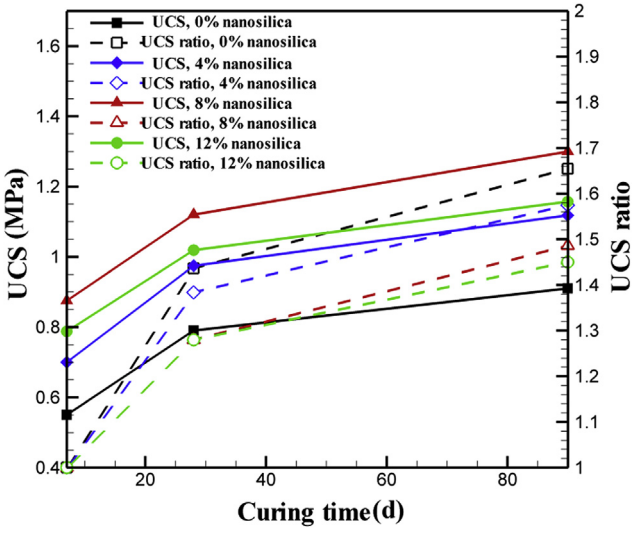

Fig. 3. Effect of curing time on the UCS of cemented sand samples with different nanosilica contents.

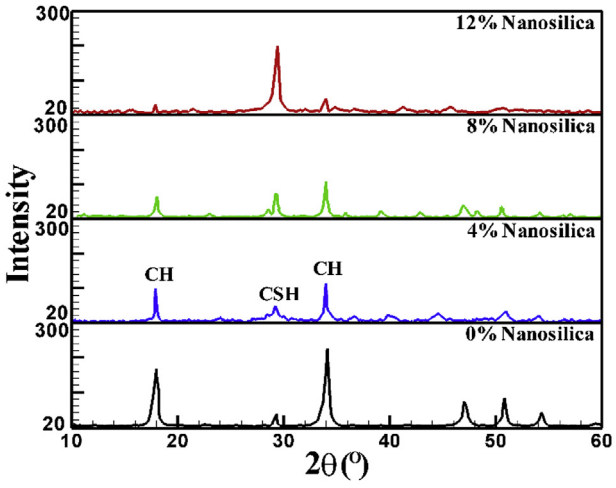

Fig. 4. Effect of nanosilica content on the XRD graph of cemented sand.

content. High nanosilica content has negative effect on cement matrix which can reduce the UCS. However, Changizi and Haddad (2015) pointed out that by adding water to sample, nanosilica produces viscous gel. The cohesion between sand grains due to viscous gel increases the UCS. Hence, under low cement content, cement matrix and viscous gel have combined effect on mechanical properties of sand sample. Therefore, the optimum nanosilica content is higher than that required for concrete design or other composite materials with highly bonded grains.

XRD analyses were performed to establish a suitable criterion for investigation of the pozzolanic activity of cemented sand samples containing nanosilica particles. Different percentages of nanosilica were added into the samples after 90 d of curing. Results for 0% and 8% of nanosilica contents were reported by Kutanaei and Choobbasti (2016b). Fig. 4 presents the XRD graphs of cemented sand samples with different nanosilica contents for 90 d of curing. For comparison, the peaks of CH at $2\theta = 18°$ and 33° and the peaks of calcium silicate hydrate (CSH) at $2\theta = 29°$ have been selected (Bahmani et al., 2014). It can be seen that the inclusion of nanosilica

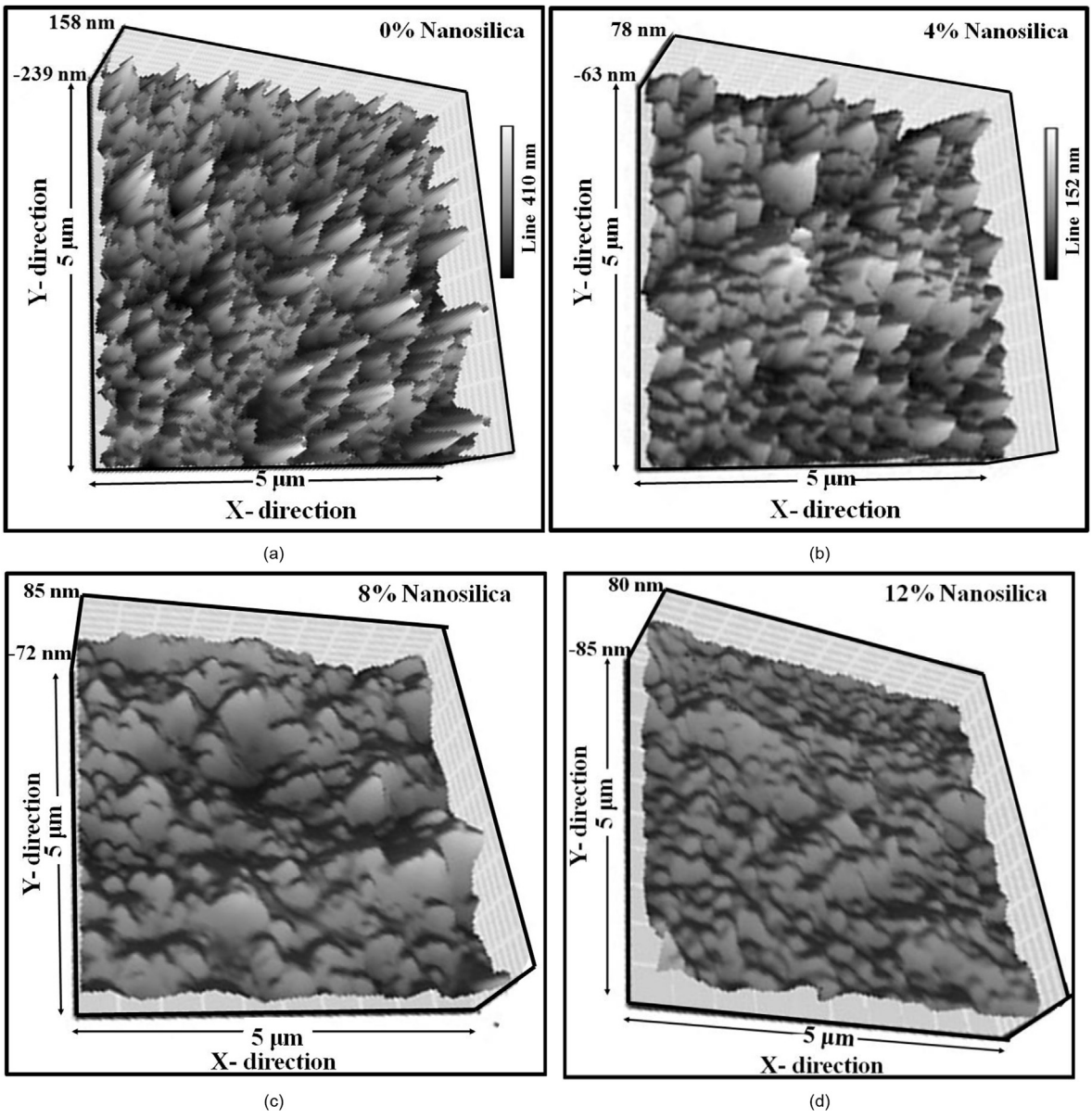

Fig. 5. AFM images of the samples for 90 d of curing: (a) 0% nanosilica, (b) 4% nanosilica, (c) 8% nanosilica, and (d) 12% nanosilica.

particles in the cemented soil increases the intensity of the CSH peaks and decreases the intensity of the CH peaks. CH crystals are hexagonal and can be arranged in the transmission zone between cement paste and sand particles, which can reduce the UCS of sand sample. In addition, previous studies showed that about 70% of hydration products are CSH gel and its average diameter is about 10 nm (Bahadori and Hosseini, 2012; Bahmani et al., 2016). Hence, the nanosilica particles can fill the pores of CSH gel matrix. Moreover, the increased nanosilica content (sample with 12% nanosilica) prevents suitable CH crystal growth, thus the CH crystal to CSH gel ratio is decreased. In the case of unsuitable CH crystal growth, no hydration reaction would occur. Hence, microcracks appear in the sample, and the UCS decreases.

AFM is a very high-resolution type of scanning probe microscopy, with demonstrated resolution in the order of fractions of a nanometer. Topography of the surface of samples with different nanosilica contents for 90 d of curing was investigated using AFM imaging. Distinct images of 5 μm × 5 μm were taken. AFM provides a true three-dimensional surface profile. Fig. 5 shows the AFM images of samples containing 6% cement and 0%, 4%, 8% and 12% nanosilica. The AFM images and topography spectra of samples show mudflat cracking and flat coherent surface layer, covering the bulk nanostructures with nanosilica particles. The homogenous and uniform structure improves the strength of the soil-cement mixture containing nanosilica comparing to the sample without nanosilica. This can be a strong evidence for promoting strength properties of soil stabilized with cement and nanosilica.

Fig. 6 shows the morphological characteristics of the cemented sand microstructure with different nanosilica contents after 90 d of curing. It can be seen that the microstructure of the mixture with 4% nanosilica is dense and uniform. The dense microstructure of sample could be induced by the high activity of nanosilica particles which increases the hydration reaction to produce more CSH gel in order to achieve higher UCS than sample without nanosilica. This has been confirmed by the unconfined compression test results. Similar results were also confirmed by tests carried out on nanosilica-enhanced composite cement pastes (Papatzani et al., 2014; Papatzani, 2016). The SEM images of the cemented sand with 8% nanosilica show the compact and dense microstructure without pores and unhydrated crystals which explains the unconfined compression test results. Moreover, Fig. 6d demonstrates that the microstructure of cemented sand with 12% nanosilica suffers from the agglomeration problem (unstable lumps). These unstable lumps make the cemented sand sample vulnerable to standing unconfined compressive loads, unlike those samples containing lower nanosilica content. The reason behind that is the high surface area of nanoparticles which makes the pozzolanic activity to form unstable lumps.

3.2.2. *Effect of curing time*

The effect of curing time on the UCS of cemented sand samples with different nanosilica contents is shown in Fig. 3. As can be seen in Fig. 3 that for all nanosilica contents, the sample with longer curing time has higher UCS. Moreover, the slope of the curve decreases with increasing nanosilica content which shows that

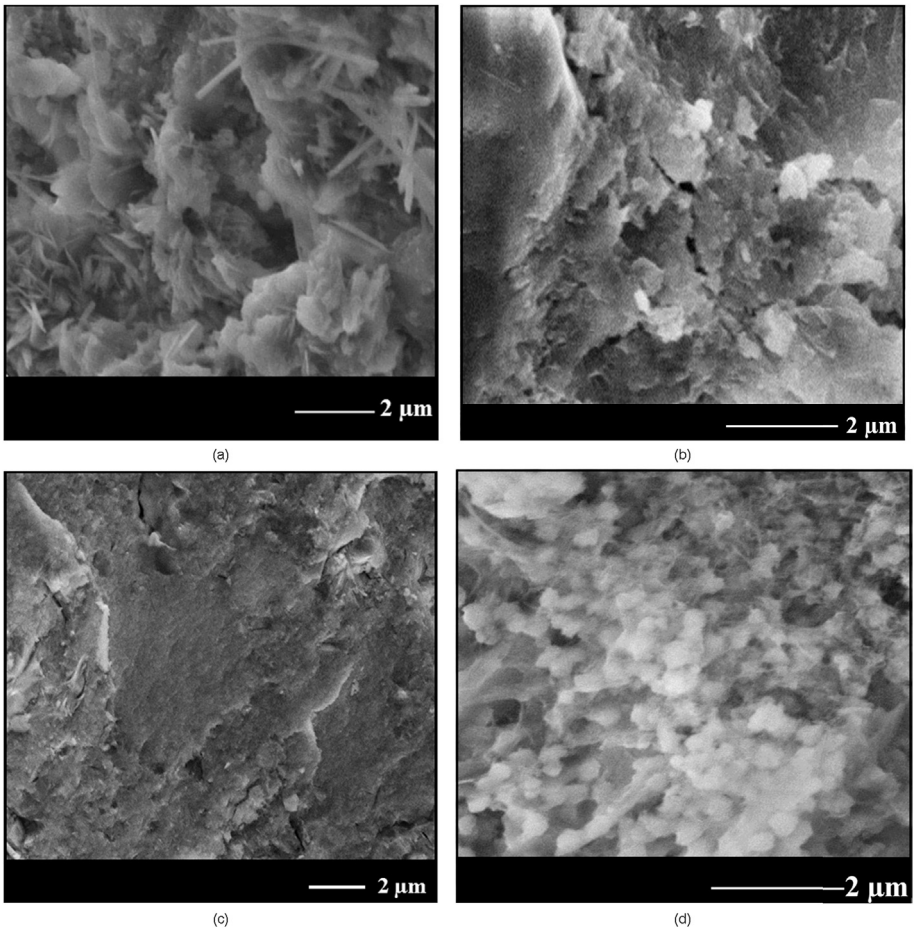

Fig. 6. SEM images of the samples for 90 d of curing: (a) 0% nanosilica, (b) 4% nanosilica, (c) 8% nanosilica, and (d) 12% nanosilica.

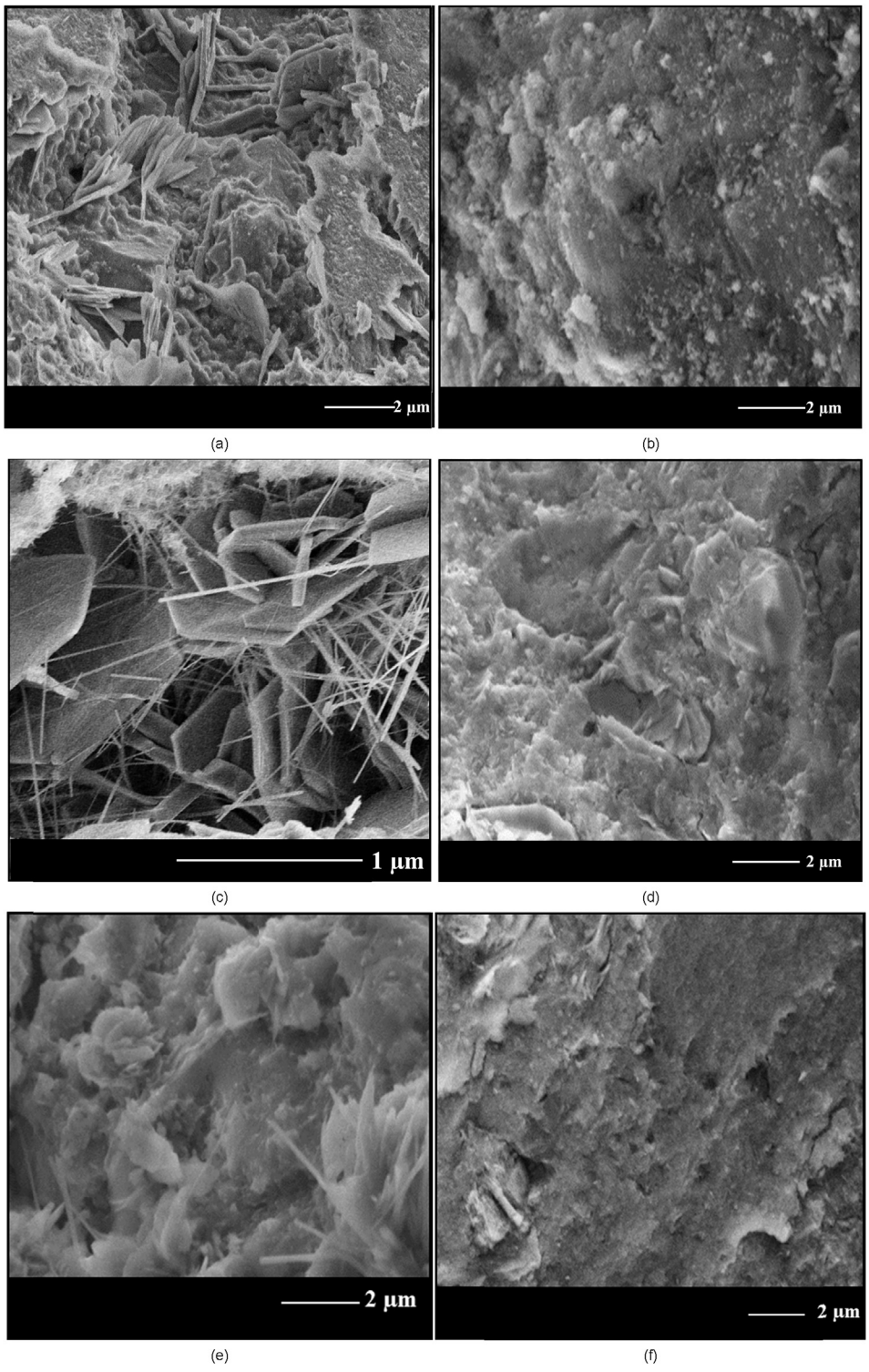

Fig. 7. Effects of curing time on the SEM images: (a) sample without nanosilica for 7 d of curing, (b) sample with nanosilica for 7 d of curing, (c) sample without nanosilica for 28 d of curing, (d) sample with nanosilica for 28 d of curing, (e) sample without nanosilica for 90 d of curing, and (f) sample with nanosilica for 90 d of curing.

increasing nanosilica content causes the cemented samples to have a faster hydration process. To interpret the rapid hydration reactions of nanosilica particles, it can be mentioned that nanoparticles have high specific surface areas, and their surfaces are very active and have numerous unsaturated bonds. Accordingly, these unsaturated bonds would initiate an intensive pozzolanic reaction between nanosilica and CH and fasten pozzolanic reactions among SiO_2 and water molecules.

SEM examinations were conducted to verify the behavior measured by the unconfined compression tests. Fig. 7a presents the SEM photo of the cement-sand mixture without nanosilica after 7 d of curing and shows a porous structure. Moreover, it can be seen

that the existence of many CH crystals is joined to the CSH gel, showing that the hydration reaction is not completed. In addition, the concentration of the CH crystals is more than that of the CSH gel. It can be also found that the CH crystal needles cover a large surface of sample. After 28 d of curing, the SEM photo in Fig. 7c demonstrates the existence of CH crystal needles and the loose structure of the cement-sand mixture without nanosilica that matches the low UCS. Fig. 7e presents the CH crystal needles, microcracks and CSH gel for the cemented sand sample after 90 d of curing. Moreover, the size and amount of the CSH after 7 d of curing have been lessened after 28 d and 90 d of curing. This explains the high UCS for the cemented sand sample after 90 d of curing in comparison to the results at the age of 7 d. Fig. 7b shows the microstructure of the cement-treated sand with 8% nanosilica after 7 d of curing. It can be seen that the microstructure of the mixture is dense with small number of CH crystals. The dense microstructure of sample at early curing time could be due to the high activity of nanosilica particles that increases the hydration reaction to produce more CSH gel in order to achieve high UCS. The SEM photo of the cemented sand with 8% nanosilica after 28 d of curing is shown in Fig. 7d. Fig. 7f shows the compact and dense microstructure without pores and unhydrated crystals which explains the unconfined compression test results. The microstructure of mixture after 90 d of curing also presents the dense and compact structure with the concentration of CSH gel in a large diameter.

4. Conclusions

This research evaluated the impacts of nanosilica particles on the mechanical characteristics and microstructure properties of cement-treated sandy soil. The obtained results can be summarized as follow:

(1) The obtained results show that when the nanosilica content is increased to an optimum amount of 8%, the UCS of the samples is improved and it then decreases with the increase in nanosilica content from 8% to 12%.
(2) The XRD results show that the inclusion of nanosilica particles in the cemented soil increases the intensity of the CSH peaks and decreases the intensity of the CH peaks. Moreover, the increased nanosilica content (sample with 12% nanosilica) prevents suitable CH crystal growth. Hence, microcracks appear in the sample, and the UCS decreases.
(3) The AFM results show that enhancing UCS with nanoparticles inclusion is primarily due to its high packing efficiency in filling pores. This can be a strong evidence for promoting strength properties of soil stabilized with cement and nanosilica.
(4) Based on the unconfined compression test results, for all nanosilica contents, the sample with longer curing time has higher UCS. Moreover, the increasing rate of UCS decreases with increasing nanosilica content which shows that increasing nanosilica content causes cemented samples to have a faster hydration process due to the higher activity of nanoparticles.
(5) The SEM results demonstrate that adding nanoparticles creates a cement-treated sand mixture with compact microstructure. It also can be concluded from the decreased amount of CH crystals that adding nanoparticles (up to optimum percentage) promotes the hydration process especially at early curing times and changes all these unhydrated crystal needles into CSH gel. In addition, the microstructure of sample with 12% nanosilica suffers from unstable lumps. These unstable lumps make the cemented sand sample vulnerable to standing unconfined compressive loads unlike those samples containing lower nanosilica content.

Conflict of interest

The authors wish to confirm that there are no known conflicts of interest associated with this publication and there has been no significant financial support for this work that could have influenced its outcome.

References

Al-Swaidani A, Hammoud I, Meziab A. Effect of adding natural pozzolana on geotechnical properties of lime-stabilized clayey soil. Journal of Rock Mechanics and Geotechnical Engineering 2016;8(5):714–25.

ASTM D2166/D2166M-16. Standard test method for unconfined compressive strength of cohesive soil. West Conshohocken, PA, USA: ASTM International; 2016.

ASTM D698. Standard test methods for laboratory compaction characteristics of soil using standard effort. West Conshohocken, PA, USA: ASTM International; 2010.

Bahadori H, Hosseini P. Reduction of cement consumption by the aid of silica nanoparticles (investigation on concrete properties). Journal of Civil Engineering and Management 2012;18:416–25.

Bahmani SH, Huat BBK, Asadi A, Farzadnia N. Stabilization of residual soil using SiO2 nanoparticles and cement. Construction and Building Materials 2014;64:350–9.

Bahmani SH, Farzadnia N, Asadi A, Huat BB. The effect of size and replacement content of nanosilica on strength development of cement treated residual soil. Construction and Building Materials 2016;118:294–306.

Changizi F, Haddad A. Strength properties of soft clay treated with mixture of nano-SiO_2 and recycled polyester fiber. Journal of Rock Mechanics and Geotechnical Engineering 2015;7(4):367–78.

Choobbasti AJ, Tavakoli H, Kutanaei SS. Modeling and optimization of a trench layer location around a pipeline using artificial neural networks and particle swarm optimization algorithm. Tunnelling and Underground Space Technology 2014;40:192–202.

Choobbasti AJ, Vafaei A, Kutanaei SS. Mechanical properties of sandy soil improved with cement and nanosilica. Open Engineering 2015;5(1):111–6.

Ghasabkolaei N, Janalizadeh A, Jahanshahi M, Roshan N, Ghasemi SE. Physical and geotechnical properties of cement-treated clayey soil using silica nanoparticles: an experimental study. The European Physical Journal Plus 2016;131(5). http://dx.doi.org/10.1140/epjp/i2016-16134-3.

Ghazi H, Baziar MH, Mirkazemi SM. Assessment of the improvement of the behavior of soil strength in the presence of nanoscale additive. Assas Journal of Science and Technology 2011;1(1):45–50 (in Persian).

Kutanaei SS, Choobbasti AJ. Triaxial behavior of fiber reinforced cemented sand. Journal of Adhesion Science and Technology 2015a;30(6):579–93.

Kutanaei SS, Choobbasti AJ. Prediction of combined effects of fibers and cement on the mechanical properties of sand using particle swarm optimization algorithm. Journal of Adhesion Science and Technology 2015b;29(6):487–501.

Kutanaei SS, Choobbasti AJ. Experimental study of combined effects of fibers and nanosilica on mechanical properties of cemented sand. Journal of Materials in Civil Engineering 2016a;28(6). http://dx.doi.org/10.1061/(ASCE)MT.1943-5533.0001521.

Kutanaei SS, Choobbasti AJ. Effects of nanosilica particles and randomly distributed fibers on the ultrasonic pulse velocity and mechanical properties of cemented sand. Journal of Materials in Civil Engineering 2016b;29(3). http://dx.doi.org/10.1061/(ASCE)MT.1943-5533.0001761.

Ladd RS. Preparing test samples using undercompaction. Geotechnical Testing Journal 1978;1(1):16–23.

Mashhadban H, Beitollahi A, Kutanaei SS. Identification of soil properties based on accelerometer records and comparison with other methods. Arabian Journal of Geosciences 2016a;9(6):1–8.

Mashhadban H, Kutanaei SS, Sayarinejad MA. Prediction and modeling of mechanical properties in fiber reinforced self-compacting concrete using particle swarm optimization algorithm and artificial neural network. Construction and Building Materials 2016b;119:277–87.

Mola-Abasi H, Shooshpasha I. Influence of zeolite and cement additions on mechanical behavior of sandy soil. Journal of Rock Mechanics and Geotechnical Engineering 2016;8(5):746–52.

Papatzani S. Effect of nanosilica and montmorillonite nanoclay particles on cement hydration and microstructure. Materials Science and Technology 2016;32(2):138–53.

Papatzani S, Paine K, Calabria-Holley J. The effect of the addition of nanoparticles of silica on the strength and microstructure of blended Portland cement pastes. In: Proceedings of the 2014 international concrete sustainability conference; 2014.

Sarokolayi LK, Beitollahi A, Abdollahzadeh G, Amreie ST, Kutanaei SS. Modeling of ground motion rotational components for near-fault and far-fault earthquake according to soil type. Arabian Journal of Geosciences 2015a;8(6):3785–97.

Sarokolayi LK, Kutanaei SS, Golafshani SM, Haji SR, Mashhadban H. Control-volume-based finite element modelling of liquefaction around a pipeline. Geomatics, Natural Hazards and Risk 2015b;7(4):1287–306.

Tavakoli H, Kutanaei SS. Evaluation of effect of soil characteristics on the seismic amplification factor using the neural network and reliability concept. Arabian Journal of Geosciences 2015;8(6):3881–91.

Asskar Janalizadeh Choobbasti is a Professor in Geotechnical Engineering, School of Civil Engineering at Babol University of Technology, Babol, Iran. He received his PhD in Geotechnical Engineering from Department of Civil Engineering, School of Engineering, the University of UMIST, UK. His research interests cover soil liquefaction, numerical modeling and ground improvement.

Saman Soleimani Kutanaei received his bachelor degree in Civil Engineering at Azad Islamic University, Ghaemshahr branch. He received his MSc degree in Geotechnical Engineering from Babol University of Technology. He is a PhD student at Babol University of Technology. His main research interests cover soil liquefaction, numerical modeling of the ground improvement, optimization using genetic algorithm and neural network, and experimental study of new concepts in civil engineering.